JOURNAL OF SOLID STATE CHEMISTRY 51, 141–151 (1984)

Characterization of the New Series of Quasi One-Dimensional Compounds $(MX_4)_nY$ (M = Nb, Ta; X = S, Se; Y = Br, I)

P. GRESSIER, A. MEERSCHAUT, L. GUEMAS AND J. ROUXEL

Laboratoire de Physicochimie des Solides, L.A. 279, 2, rue de la Houssinière, 44072 Nantes Cédex, France

AND P. MONCEAU

Centre de Recherches sur les Très Basses Températures, CNRS, B.P. 166X, 38042 Grenoble Cédex, France

Received June 14, 1983; in revised form September 14, 1983

A detailed investigation on the new series of compounds $(MX_4)_nY$ (M = Nb, Ta; X = S, Se; Y = Br, I) is given through structural information and resistivity measurements. All these compounds are built with the same framework which is composed of MX_4 chains and halogen atoms between these chains. It is found that the resistivity behavior is closely related to the metal–metal sequence along the MX_4 chain.

Introduction

The low-dimensional character of a structure reflects directly a strong anisotropy in chemical bonding. The corresponding compounds can be regarded as being composed of layers or chains, the internal cohesion of which is due to strong iono-covalent or metallic bonds. In contrast, interlayer or interchain bonds are very weak and generally of the van der Waals type.

Chalcogen-rich niobium and tantalum chalcogenides provide good examples of solids with low dimensionality. The dichalcogenides have been important model solids illustrating the physics and chemistry of two-dimensional materials. However, more recently, the preparation and characterization of $NbSe_3$ (*1*) opened up a new field of interest in one-dimensional investigations.

For both MX_2 and MX_3 compounds, such as $NbSe_2$ and $NbSe_3$, the same trigonal prismatic coordination around the metal atom is observed. In the case of $NbSe_2$, the prisms are arranged in $[NbSe_2]$ infinite layers, whereas for $NbSe_3$ they are stacked on top of each other in order to form $[NbSe_3]$ infinite chains, as shown in Fig. 1. The latter framework provides trichalcogenides with a pseudo one-dimensional behavior, as exemplified by the remarkable charge density wave (CDW) phenomena observed in $NbSe_3$ (*2*).

The presence of anionic pairs $(X_2)^{2-}$ in trichalcogenides makes them different from dichalcogenides. Formally, NbX_3 may be formulated as Nb^{4+} $(X_2)^{2-}$ X^{2-}. The metal configuration (d^1) may lead to formation of metal–metal pairs along the chain, determining a semiconducting behavior as observed in NbS_3 type I with E = 0.44 eV (*3*).

0022-4596/84 $3.00

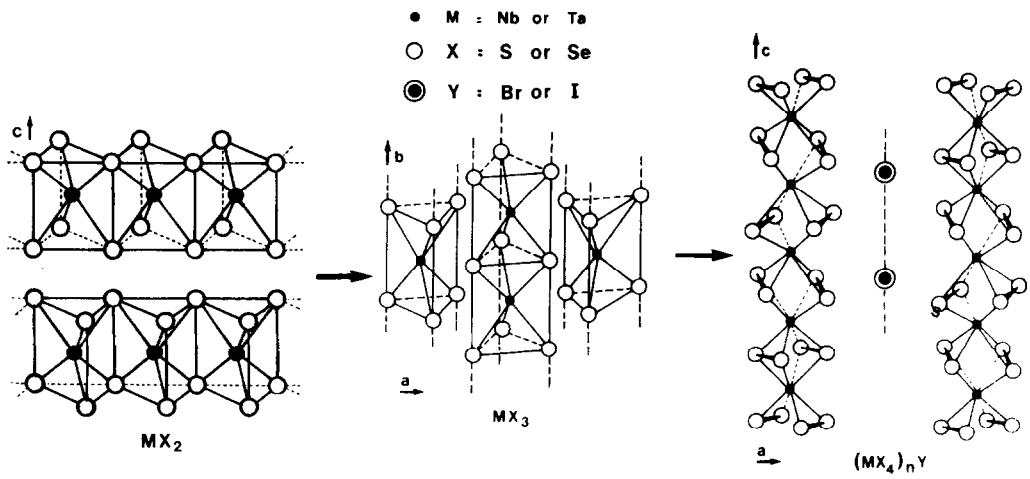

FIG. 1. MX_2, MX_3, and MX_4 schematic models.

Moreover, anionic pairs exhibit various bond lengths which allows trichalcogenides to be classified as a function of the number (n) of different $[MX_3]$ chains, with each chain corresponding to a particular $[X_2]^{2-}$ pair length ($ZrSe_3$ type: $n = 1$, $TaSe_3$ type: $n = 2$, $NbSe_3$ type: $n = 3$). In these compounds, $(X_2)^{2-}$ pairs clearly behave as "electron reservoirs." Depending upon their lengths, they give different electrical properties to the metallic chain (Nb or Ta).

In 1977, the $(NbSe_4)_3I$ compound was characterized (*4*). From a structural point of view this compound could be related to a pseudo one-dimensional model (see Fig. 1) with a niobium chain confined within a rectangular antiprismatic framework of $(Se_2)^{2-}$ pairs. Iodine atoms lie between these $(NbSe_4)_\infty$ columns, as shown in Fig. 2. Similar derivatives, $(MSe_4)_nBr$, with M = Nb or Ta, were obtained (*5*). The common feature of tri- and tetrachalcogenides was the occurrence of metallic chains and chalcogen pairs. In the present work, we show that we are dealing with a new series of materials with general the formula $(MX_4)_nY$ (M = Nb, Ta; X = S, Se; Y = Br, I). New materials are characterized and a general discussion of these compounds and a comparison with trichalcogenides are given.

I. $(NbSe_4)_3I$ Structural Type: Characterization and Discussion

Single, needle-shaped crystals of this phase were obtained by mixing the starting elements in an evacuated and sealed glass tube at temperatures ranging from 400 to 550°C. $(NbSe_4)_3I$ crystallizes with tetragonal symmetry, space group *P4/mnc*. The unit cell parameters are $a = 9.489(1)$ Å and $c = 19.13(3)$ Å. The structure (*4*) is composed of $[NbSe_4]$ chains and iodine columns which are both directed parallel to the c axis. Two niobium atoms having the same z value, but belonging to different chains, are 6.70 Å apart. Along the chains, six niobium atoms are located within one c parameter (see Fig. 2). Two different Nb–Nb distances (3.06 and 3.25 Å) occur along this axis. Each short Nb–Nb bond is followed by two longer Nb–Nb distances, i.e., -Nb-3.06-Nb-3.25-Nb-3.25-Nb-3.06-Nb. The niobium coordination is a rectangular antiprism composed of four $(Se_2)^{2-}$ pairs. The dimensions of each rectangle are about 3.5

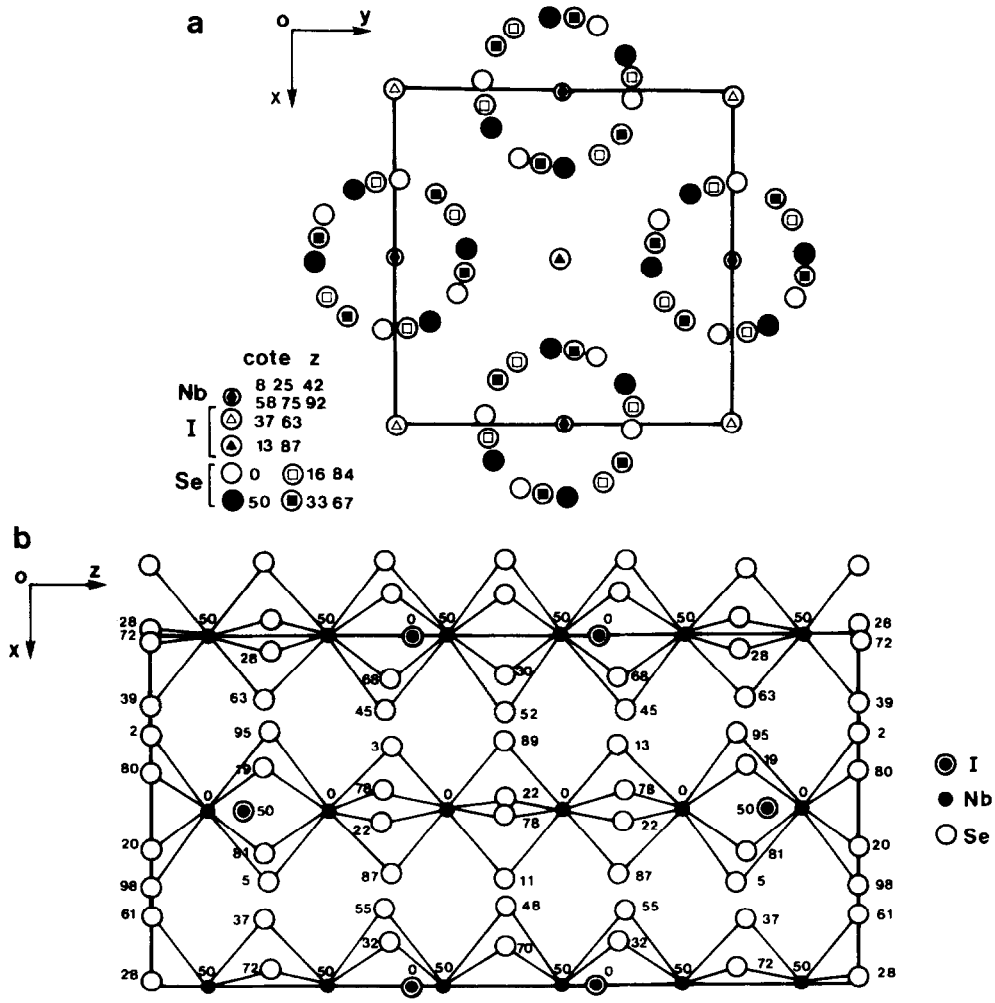

FIG. 2. (a) Projection of $(NbSe_4)_3I$ structure on to the $xy0$ plane. (b) Projection of $(NbSe_4)_3I$ structure on to the $x0z$ plane.

and 2.35 Å, the latter value corresponding to the typical $(Se_2)^{2-}$ pairing. The antiprisms are stacked along the c axis in a screw-like arrangement. The iodine atoms are located in the channels between the $[NbSe_4]$ chains (Fig. 2).

A simple model can be proposed for the niobium sequence. The short Nb–Nb distance could be a consequence of a Nb^{4+}–Nb^{4+} bond (d^1–d^1 configuration). These pairs are separated by a Nb^{5+} cation (d^0 configuration), which produces two longer Nb–Nb distances. This agrees with the formula $2Nb^{4+}Nb^{5+}$ $6(Se_2)^{2-}I^-$. We can formally consider iodine atoms as isolated I^- species because the shortest I–I distance is 4.96 Å, which is very long compared to 2.68 Å in solid I_2 and a maximum of 3.07 Å in I_3^-.

XPS measurements were performed on this compound using an AEI-ES-200 apparatus. A glove box with a controlled N_2 atmosphere was attached to it. Spectra were recorded with monochromatic AlK_α radiation (energy = 1486.6 eV, width = 0.4 eV).

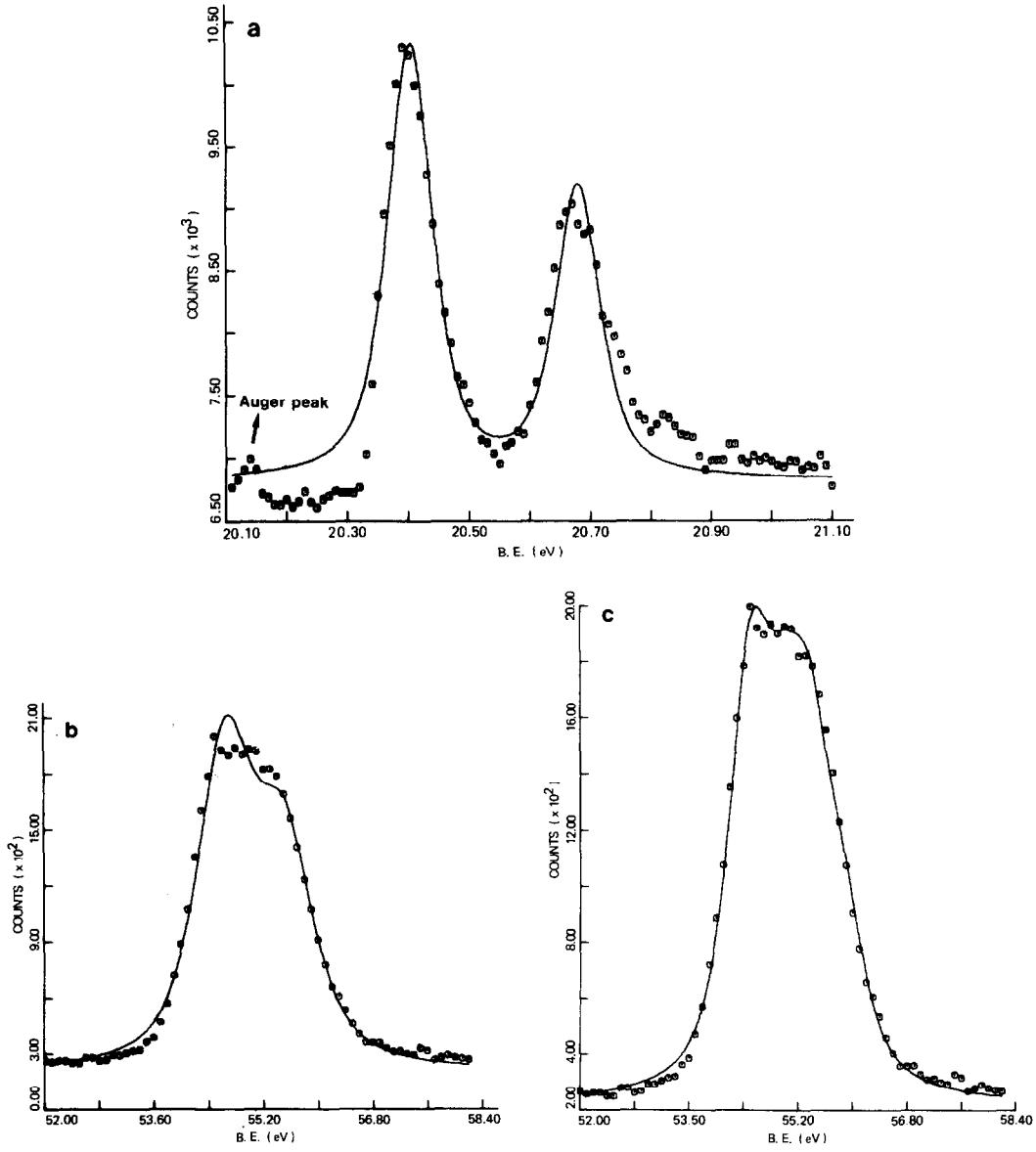

FIG. 3. (a) Nb 3*d* spectrum in $(NbSe_4)_3I$. (b) Se 3*d* spectrum in $(NbSe_4)_3I$. The fit was obtained with only one sort of selenium atoms. (c) Se 3*d* spectrum fitted with two sorts of selenium atoms (see Table I).

Samples were crushed on an indium foil to avoid charging problems. To ensure a well-defined Fermi level versus energy scale, an Ag calibration spectrum was taken before and after measurements. According to our assumption, one should expect some mixed-valence effects in the Nb 3*d* spectrum, possibly even the occurrence of two signals in a 2 : 1 ratio corresponding to formal valences of 4 and 5, respectively. The monochromatized Nb 3*d* spectrum (see Fig. 3a), however, shows a quite normal

TABLE I

PARAMETERS USED IN THE FIT OF Nb AND Se 3*d* SPECTRA

		B.E.	*W*	*I*	
Se_2^{2-}	3*d* 3/2	55.36	0.77	4	
	3*d* 5/2	54.49	0.77	6	
$Se^{(-1+\delta)}$	3*d* 3/2	55.86	0.77	2	
	3*d* 5/2	54.99	0.77	3	
$Nb^{4+\delta'}$	3*d* 3/2	206.79	0.88	2	
	3*d* 5/2	204.02	0.88	3	
I^-	3*d* 3/2	617.8	1.7	2	Non-monochromated
	3*d* 5/2	629.3	1.7	3	

Note. B.E. is the binding energy (in eV). *W* is the width and *I* the intensity of the signal.

narrow peak (0.88 eV). The Nb level does not indicate any mixed-valence effects either because

(i) there is no mixed valency,

(ii) the degree of delocalization is too high,

(iii) the Nb 3*d* level is too insensitive to mixed-valence effects.

The Se 3*d* spectrum does show an anomalous shape. The best fit of the spectrum (see Figs. 3b,c) is obtained for two Se signals in a 2 : 1 ratio. The binding energy separation between them is quite large (0.5 eV) (see Table I). The difference in the environment of selenium atoms may explain this splitting, since one-third of all Se atoms have a neighboring I atom at 3.27 Å, which is shorter than the sum of van der Waals' radii. Hence an electronic transfer can occur, which gives a formal valence of $(-1 + \delta)$ rather than (-1) to the Se atoms.

Resistivity measurements were performed by a four-probe method using a low-frequency bridge (33 Hz). Contacts were made with knotted gold wire around the single crystal and bonded with gold paint to minimize the contact resistances. Measurements were performed between 77 and 500 K. The resistivity curves (Figs. 4a,b) of $(NbSe_4)_3I$ indicate semiconducting behavior above room temperature with a gap of 0.19 eV. The room-temperature resistivity is about 1 $\Omega \cdot$ cm. Around 275 K we measure a sharp decrease of the activation energy. At lower temperatures two types of behavior have been observed. The corresponding crystals cannot be distinguished by X-ray

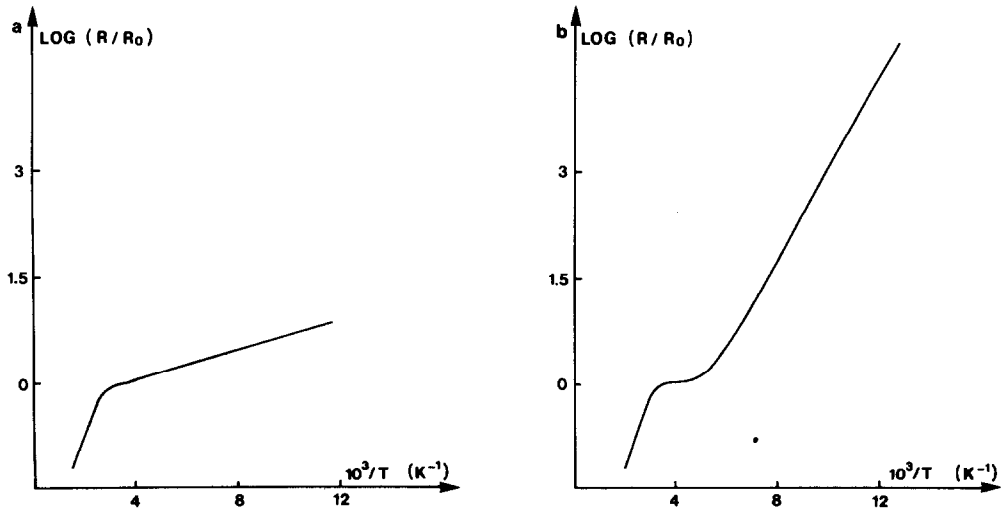

FIG. 4. (a) Log R/R_0 versus $10^3/T$ for $(NbSe_4)_3I$ type I compound. (b) Log R/R_0 versus $10^3/T$ for $(NbSe_4)_3I$ type II compound.

TABLE II

UNIT CELL PARAMETERS FOR IODINE TETRASELENIDES

$(NbSe_4)_3I$	$(NbSe_4)_{3.33}I$
a = 9.489(1) Å	a = 9.464(1) Å
c^a = 19.13 (3) Å	c^a = 31.910(8) Å
V = 1722.48 Å^3	V = 2858.09 Å^3
Tetragonal *P4/mnc*	Tetragonal *P4/mcc*
Z = 4	Z = 6
$(TaSe_4)_3I$	$(TaSe_4)_2I$
a = 9.4767(7) Å	a = 9.5317(9) Å
c^a = 19.071 (3) Å	c^a = 12.761 (3) Å
V = 1712.72 Å^3	V = 1159.38 Å^3
Tetragonal *P4/mnc*	Tetragonal *I422*
Z = 4	Z = 4

[a] Growing axis.

techniques; they both present the characteristics of $(NbSe_4)_3I$. The measurements have been reproduced at least three times on different crystals of both types. Type I behavior is characterized by a very small semiconducting gap below 275 K (Fig. 4a). In type II crystals, after the decrease of the gap near 275 K, the resistivity increases again at lower temperatures, showing once more a typical semiconducting behavior (E = 0.11 eV) (Fig. 4b).

II. New Related Iodine Compounds

By changing the relative amounts of the reacting elements or by replacing niobium with tantalum, three new compounds related to $(NbSe_4)_3I$ have been obtained. Table II summarizes the unit cell parameters. All of the compounds have two (MX_4) chains per unit cell (similar a values). They differ by the c parameter and the corresponding metal–metal sequence in the MX_4 chains.

(*1*) $(TaSe_4)_2I$

$(TaSe_4)_2I$ was prepared by direct combination of the elements in sealed silica tubes at temperatures ranging from 850 to 900 K. The detailed structure of this material has already been published (*6*) and shows a c parameter which is two-thirds that of $(NbSe_4)_3I$ (see Table II). An important point is that the tantalum–tantalum distances in each chain are all identical (3.206 Å). The room-temperature resistivity is 1.5×10^{-3} $\Omega \cdot$ cm, which is lower than those for the previous compounds. Figure 5 shows $\log(R/R_0)$ versus T^{-1}. A transition, which is located at 263 K and is magnified by the derivative curve, corresponds to the appearance of a semiconducting state (E = 0.25 eV). This transition has a CDW origin. This clearly appears in the nonlinear transport properties that are measured below the transition temperature. Figure 6 shows the

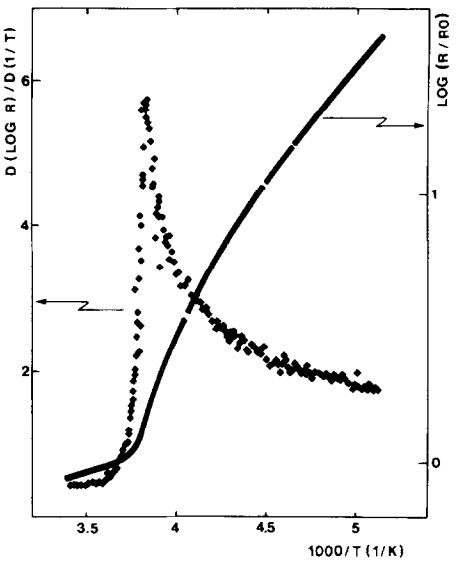

FIG. 5. Log R/R_0 versus $10^3/T$ for $(TaSe_4)_2I$.

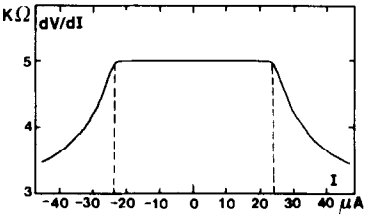

FIG. 6. Nonlinear effects observed for $(TaSe_4)_2I$ at 240.8 K. Critical current I = 25 μA (E_c = 1.5 V cm^{-1}).

variation of the differential resistance, dV/dI, as a function of the applied current at 240.8 K. Above a critical current of 25 μA ($E = 1.5$ V · cm^{-1}), the drop in the differential resistance shows that Ohm's law is no longer obeyed. Such behavior, first observed in the case of $NbSe_3$ (*7*), is a consequence of the depinning of the CDW above a critical field. Preliminary electron-diffraction experiments confirm the CDW state (*8*).

(*2*) $(TaSe_4)_3I$

This material is very similar to $(NbSe_4)_3I$ (Table II). The room-temperature resistivity is about 0.2 Ω · cm. Again it is two orders of magnitude higher than that for $(TaSe_4)_2I$, in agreement with the highly probable succession of long and short distances in a structure like $(NbSe_4)_3I$. Up to now the quality of the crystals has not permitted an investigation of their physical properties.

Chemical microprobe analysis of a single crystal gives for Ta, exp. 33.6% (theor. 33.56%); for Se, exp. 58.8% (theor. 58.59%); for I, exp. 7.7% (theor. 7.85%).

(*3*) $(NbSe_4)_{3.33}I$

Originally, $(NbSe_4)_{3.33}I$ crystals were picked from preparations made in an attempt to obtain $MgNb_3Se_{10}$. To do that, mixtures of the elements in stoichiometric proportions were heated at 900–1000 K in sealed silica tubes with iodine as the transport agent. The structure of $(NbSe_4)_{3.33}I$ is closely related to that of $(NbSe_4)_3I$ though more complex in the details. The complete structural study will be published later. It appears that, in agreement with a c parameter which is 10/6 times that of $(NbSe_4)_3I$, there are 10 niobium atoms along each (MX_4) chain in a unit cell. The chemical formula comes from this structural study. It appears as $Nb_{10}Se_{40}I_3$, to be compared with $Nb_6Se_{24}I_2$ for $(NbSe_4)_3I$. Microprobe analysis on single crystals (Microsonde Ouest-CNEXO) gave for Nb, exp. 20.83% (theor. 20.79%); for Se, exp. 71.03% (theor. 70.68%); for I, exp. 8.13% (theor. 8.52%).

The alternation of long and short distances now becomes -Nb-3.17-Nb-3.17-Nb-3.23-Nb-3.15-Nb-3.23-Nb-3.17-. The difference between long and short distances is much smaller than in $(NbSe_4)_3I$. This may explain why the room-temperature resistivity of $(NbSe_4)_{3.33}I$ is about 1.5×10^{-2} Ω · cm, which is two orders of magnitude less than that for $(NbSe_4)_3I$. In addition, the temperature variation of the resistivity, which agrees with a thermal activated mechanism ($E = 0.13$ eV) at lower temperature (see Fig. 7), shows a transition at 272 K (see derivative curve). Once more this type of curve strongly recalls that of many one-dimensional systems, particularly TaS_3, which undergo a metal–insulator transition at low temperatures ($T = 240$ K in monoclinic TaS_3 (*9*), $T = 215$ K in orthorhombic TaS_3 (*10*)), and $(TaSe_4)_2I$. Indeed, as in the case of $(TaSe_4)_2I$ preliminary experiments under various electrical fields show nonlin-

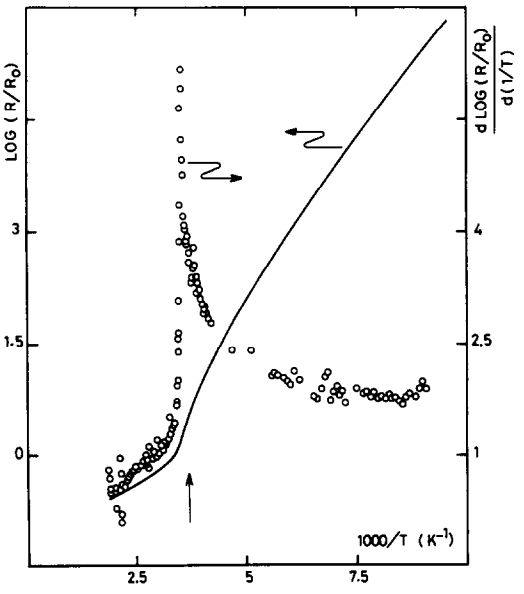

FIG. 7. Log R/R_0 versus $10^3/T$ for $(NbSe_4)_{3.33}I$.

TABLE III

UNIT CELL PARAMETERS OF OTHER HALOGEN TETRACHALCOGENIDES

Sulfide derivatives

$(NbS_4)_4Br$	$(NbS_4)_4I$
a = 17.843(3) Å α = 99.19(1)°	a = 17.857(3) Å α = 99.00(1)°
b^a = 24.938(4) Å β = 104.46(1)°	b^a = 24.927(5) Å β = 104.73(1)°
c = 13.405(2) Å γ = 131.32(1)°	c = 13.498(2) Å γ = 130.84(1)°
V = 3881.7 Å^3	V = 3948.2 Å^3
Triclinic $P\bar{1}$	Triclinic $P\bar{1}$
Z = 8	Z = 8

Selenide derivatives

$(NbSe_4)_4Br$	$(NbSe_4)_3Br$	$(TaSe_4)_4Br$
a^a = 2 × 12.930(2) Å	a^a = 3 × 12.930(2) Å	a^a = 12.841(2) Å
b = 24.258(3) Å	b = 24.937(2) Å	b = 13.875(2) Å
c = 28.355(3) Å	c = 28.482(3) Å	c = 20.360(4) Å
β = 131.67(1)°	β = 131.12(1)°	β = 141.43(1)°
V = 2 × 6643.3 Å^3	V = 3 × 6664.1 Å^3	V = 2261.9 Å^3
Monoclinic $P2_1/c$	Monoclinic $P2_1/c$	Monoclinic $P2_1/c$
Z = 12 × 2	Z = 12 × 3	Z = 4

[a] Growing axis.

ear effects. This favors a CDW-type transition which should be confirmed by electron-diffraction experiments.

III. Bromine Tetraselenides, Iodine and Bromine Tetrasulfides

(1) *Bromine Tetraselenides*

Preparation and structural discussion of these compounds have already been reported (*5*). Their unit cell parameters are listed in Table III. Bromine tetraselenides are less symmetrical than their iodine analogs. A 2a-type superstructure is observed for $(NbSe_4)_4Br$, whereas $(NbSe_4)_3Br$ exhibits a 3a-type superstructure.

There are chains of four niobium atoms (a = 12.93 Å) in a subcell, and bromine atoms located in the resulting tunnels are responsible for the superstructure. Our structural hypothesis about $(NbSe_4)_4Br$ presumes that the alternation is two short (3.15 Å) and two long (3.45 Å) distances and that niobium atoms are not exactly aligned.

A bromine–tantalum derivative $(TaSe_4)_4Br$ was also obtained. The unit cell parameters are reported in Table III.

These compounds are semiconducting; the energy gap and room-temperature resistivities are:

	E_g (eV)	ρ_{RT} ($\Omega \cdot$ cm)
$(NbSe_4)_4Br$	0.36	50
$(NbSe_4)_3Br$	0.25	8
$(TaSe_4)_4Br$	0.18	3.5

(2) *Halogen Tetrasulfides of Niobium* $(NbS_4)_nY$ (Y = *Br, I*)

Unfortunately, we were not able to prepare halogen tetrasulfides of tantalum, but only those of niobium. Each batch contained several small crystals. Due to their small mass, chemical analysis is not precise enough, which makes it difficult to ascertain their chemical composition. In addition, the distorted structural type (triclinic $P\bar{1}$) cannot be used to predict the chemical composition by referring to the previous

TABLE IV

MICROPROBE ANALYSIS (MICROSONDE OUEST-CNEXO) OF SINGLE CRYSTALS OF THE NEW SULFIDE DERIVATIVES WITH UNDETERMINED STRUCTURES AND DENSITY MEASUREMENTS (CORRECTED WEIGHT FRACTION %)

$(NbS_4)_{32}Br_{10}$			$(NbS_4)_{32}I_8$		
	exp.	theor.		exp.	theor.
Nb	38.1	37.75	Nb	36.5	36.74
S	52.1	52.10	S	50.9	50.72
Br	9.8	10.14	I	12.2	12.54
ρ (g/cm^3)	3.35	3.37	ρ (g/cm^3)	3.41	3.40

compounds. Nevertheless, from microprobe analysis and density measurements (Table IV), the composition is estimated to be close to those of $(NbS_4)_{32}Br_{10}$ and $(NbS_4)_{32}I_8$, respectively. The high room-temperature resistivities (ρ_{RT}) of both compounds are $2 \times 10^6\ \Omega \cdot$ cm for $(NbS_4)_nI$ and $4 \times 10^8\ \Omega \cdot$ cm for $(NbS_4)_nBr$.

Discussion

The $(MX_4)_nY$ phases represent a series of new pseudo one-dimensional materials with very promising electrical properties, the most interesting point being the nonlinear effects which are observed in the cases of $(TaSe_4)_2I$ and $(NbSe_4)_{3.33}I$.

Including the four new compounds prepared in this work, nine $(MX_4)_nY$ compounds are known, which allows at first a general structural discussion and will provide a basis for an interpretation of the electrical properties. All the compounds refer to the same structural model, built from $(MX_4)_\infty$ chains and halogen columns, parallel to the growing axis. The ordered distribution of the halogen atoms in these columns induces superstructures which are commensurate with the arrangement of Nb or Ta atoms in the MX_4 chains. The $(MX_4)_nY$ structure differs from the VS_4 type (*11*) by the presence of the halogen and by the variety of metal–metal bonds along the metallic chain. Table V shows the various metal–metal sequences in the different compounds.

The d^1 electron of the M^{4+} ions either can be involved in a strong d^1–d^1 bond as found in Nb_2Se_9 (*12*), where the short Nb–Nb distance is equal to 2.89 Å, which results in a semiconducting behavior (e.g., Nb_2Se_9, E = 0.78 eV) or can be more or less delocalized giving rise possibly to a metallic conductivity. When a pairing occurs it has to be associated with the shortest M–M distance. In $(NbSe_4)_3I$, the corresponding Nb–Nb distance, i.e., 3.06 Å, fits very well with the value of 3.037 Å observed in NbS_3 (*3*). The occurrence of M^{4+} ($4d^1$) in pairs $(M$–$M)^{8+}$ is the result of a strong interaction between the metal (dz^2) orbitals, as these

TABLE V

VARIOUS METAL–METAL SEQUENCES IN THE $(MX_4)_nY$ COMPOUNDS

Compound	M–M sequence	ρ_{RT} ($\Omega \cdot$ cm)	E (eV)
$(NbSe_4)_3I$	___Nb$\overline{3.25}$Nb$\overline{3.25}$Nb$\overline{3.06}$Nb___	1	0.19 at RT
$(NbSe_4)_{3.33}I$	___Nb$\overline{3.17}$Nb$\overline{3.17}$Nb$\overline{3.23}$Nb$\overline{3.15}$Nb$\overline{3.23}$Nb___	10^{-2}	0.13
$(TaSe_4)_2I$	___Ta$\overline{3.206}$Ta$\overline{3.206}$Ta___	1.5×10^{-3}	0.25
$(TaSe_4)_3I$	(same sequence as for $(NbSe_4)_3I$)	0.2	?
$(NbSe_4)_4Br$	___Nb$\overline{3.15}$Nb$\overline{3.15}$Nb$\overline{3.45}$Nb$\overline{3.45}$Nb___	50	0.36
$(NbSe_4)_3Br$	?	8	0.25
$(TaSe_4)_4Br$	?	3.5	0.18

orbitals are mainly directed along the metal chain. The interaction leads to a bonding A_g (dz^2) level occupied by two electrons, the other d orbitals being empty. The electrical properties along the chain also depend on the presence of M^{5+} ions with a d^0 configuration which should interrupt a metallic conductivity.

Of course these are extreme models. Besides the fact that M^{5+} ions are not to be expected for niobium and tantalum in the presence of selenium, the observation of various types of distances in the different compounds shows that intermediate situations are occurring.

In those compounds exhibiting a semiconducting behavior the associated activation energies are functions of the difference between long and short metal–metal distances (Table V). The more homogeneous the distances are, the lower the activation energy. This is in accordance with a hopping mechanism. Experiments under pressure are in project.

When the metal–metal distances are equal, a high conductivity state is observed at room temperature and a transition toward a semiconducting state is observed in $(TaSe_4)_2I$ at 263 K. This transition is associated with a CDW as proved by the nonlinear effects observed above critical fields (for example 1.5 V · cm^{-1} at 241 K) and by preliminary electron-diffraction studies (*8*).

An important point concerns the decrease of the semiconducting energy gap in type I and type II $(NbSe_4)_3I$ crystals, measured around 275 K, and common to both type of crystals. This behavior is unusual. It leads to a higher conducting state when lowering the temperature. It supposes a modification of the available electronic density along the metallic chains. A reasonable explanation is the formation of $(I_3)^-$ ions from isolated I^- ions along the iodine columns. This would result in a two-thirds decrease of the number of Nb^{5+} (d^0) ions along the metallic chain and a corresponding increase of the electronic population able to be delocalized along this chain. A vibrational study is in progress and should confirm this model. The formation of $(I_3)^-$ ions is possible from a geometrical point of view and is also suggested by the anisotropy ellipsoids of I^- ions in the $(NbSe_4)_3I$ structure (*4*). Type I crystals do not undergo any other transition when the temperature is lowered further. We think that these crystals represent stoichiometric $(NbSe_4)_3I$ crystals. On the contrary, in type II crystals, after the anomaly of resistivity at about 275 K, there is a return to a semiconducting state. The activation energy observed in the low temperature region (0.13 eV) is very close to that of $(NbSe_4)_{3.33}I$ (0.11 eV). This suggests that type II crystals could present microdomains of the $(NbSe_4)_{3.33}I$ composition. Without any modification of the structural framework this would simply result in different local arrangements of iodine ions. These domains which act as local defects perpendicular to the chain axis are statistically distributed (no X-ray effect) and certainly few because they do not imply a significant composition variation within chemical analysis accuracy. One way to verify the correctness of this hypothesis consists of studying the possible physical behavior of type II crystals when heated under iodine pressure. A type I crystal behavior should be observed. Experiments are currently underway.

Acknowledgments

XPS measurements were performed at the University of Groningen (Holland). One of us (A.M.) would like to thank Professor Jellinek and Professor Sawatsky for useful help in discussions and experiments.

References

1. A. Meerschaut and J. Rouxel, *J. Less-Common Met.* **39,** 197 (1975).
2. P. Monceau, J. Richard, and M. Renard, *Phys. Rev. B* **25,** 931 (1982); J. Richard, P. Monceau, and M. Renard, *Phys. Rev. B* **25,** 948 (1982).

3. J. RINJSDORP AND F. JELLINEK, *J. Solid State Chem.* **25,** 325 (1978); M. NUNEZ-REGUEIRO, *Thèse 3° cycle,* University of Grenoble (1979).
4. A. MEERSCHAUT, P. PALVADEAU, AND J. ROUXEL, *J. Solid State Chem.* **20,** 21 (1977).
5. L. GUEMAS, P. GRESSIER, A. MEERSCHAUT, D. LOUER, AND D. GRANDJEAN, *Rev. Chim. Miner.* **18,** 91 (1981).
6. P. GRESSIER, L. GUEMAS, AND A. MEERSCHAUT, *Acta Crystallogr. B* **38,** 2877 (1982).
7. P. MONCEAU, N. P. ONG, A. M. PORTIS, A. MEERSCHAUT, AND J. ROUXEL, *Phys. Rev. Lett.* **37,** No. 10, 602 (1976).
8. C. ROUCAU AND R. AYROLES, private communication.
9. C. ROUCAU, R. AYROLES, P. MONCEAU, L. GUEMAS, A. MEERSCHAUT, AND J. ROUXEL, *Phys. Status Solidi* **62,** 483 (1980).
10. T. SAMBONGI, K. TSUTSUMI, Y. SHIOZAKI, M. YAMAMOTO, K. YAMAYA, AND Y. ABE, *Solid State Commun.* **22,** 729 (1977).
11. R. ALLMAN, I. BAUMAN, A. KUTOGLU, H. ROSCH, AND E. HELLNER, *Naturwissenschaften* **51**(11), 263 (1964); A. KUTOGLU AND R. ALLMAN, *Neues Jahrb. Mineral. Monatsh.* **8,** 339 (1972).
12. A. MEERSCHAUT, L. GUEMAS, R. BERGER, AND J. ROUXEL, *Acta Crystallogr. B* **35,** 1747 (1979).